17th World Conference on Earthquake Engineering, 17WCEE
Sendai, Japan - September 13th to 18th 2020

RESILIENCE ASSESSMENT OF A BUILDING CONSIDERING THE EFFECTS OF AFTERSHOCKS

C. Zhai[(1)] , W. Wen[(2)] , D. Ji[(3)]

[(1)] *Professor, School of Civil Engineering, Harbin Institute of Technology, zch-hit@hit.edu.cn*
[(2)] *Assistant Professor, School of Civil Engineering, Harbin Institute of Technology, wenweiping@hit.edu.cn*
[(3)] Assistant Professor, School of Civil Engineering, Harbin Institute of Technology, jiduofa@hit.edu.cn

Abstract

The massive economic losses induced by earthquakes have long-term and serious impacts on the economic and social development. For improving the overall earthquake prevention and mitigation capabilities, system seismic resilience has become the research highlight in earthquake engineering which includes the damage assessment, government responses and recovery process. However, few studies focused on the effect mainshock-aftershock (MSAS) sequences on the seismic resilience of systems. Aftershocks usually follow the mainshock of an earthquake and have the potential to induce additional damage in the mainshock-damaged structures. Besides, the occurring of aftershocks would significantly affect the repair and recovery of a damaged structure, and thus further affect the resilience of a structure. This paper intends to assess the seismic resilience of a building considering the effects of aftershocks. The recovery time and pre-event functionality are introduced in the definition of the resilience loss factor which make it concentrate more on the intrinsic characteristics of structures during the recovery process. A reinforced concrete (RC) frame structure designed according to the current Chinese seismic code is demonstrated for the evaluation of resilience loss incorporating MSAS sequences. The structure is modeled with the OpenSees where columns and beams are simulated by the displacement-based beam-column elements with nonlinear fiber section. Then, increment dynamic analysis is applied to obtain the seismic demand of structure and maximum inter-story drift ratio (MIDR) is utilized to quantify the damage of this structure under MSAS sequences. The spectral acceleration (Sa) of mainshock ground motion is scaled from 0.1 g to 1.2 g, and relative intensity of the corresponding aftershock ground motion (i.e., ratio of the aftershock Sa to the mainshock Sa) is scaled to 0.5, 0.8 and 1.0 respectively. The cost of this building is computed based on the construction project cost information provided by the department of housing and urban-rural development of China. The economic losses induced by MSAS sequences are assessed by the damage extent and the loss ratios of various damage states provided by the code of the earthquake field work. The numerical results of case study illustrate that replacement threshold and aftershocks have a significant effect on resilience loss. The resilience loss of structure can exceed 200% and 400% considering replacement threshold and aftershocks respectively. The proposed resilience loss factor can be used to design a new structure by controlling the level of resilience loss and assess the seismic resilience of a building considering the effect of replacement threshold and aftershocks.

Keywords: resilience, aftershock, recovery, economic loss

1. Introduction

The seismic resilience of a structure or community is a critical part in the field of earthquake engineering. The recovery process and the earthquake-related consequences (e.g. damage stage, direct economic loss) in the post-earthquake environment have an great influence on the economy and society.

Recent years, some researchers developed some conceptual frameworks for quantifying seismic resilience of a community or a system. [1-9] These frameworks were proposed generally from the point of view of community or system. Besides, many investigations studied the earthquake resilient structures by introducing new type of structural systems or components, such as employing controlled rocking on steel braced-frame system, installing energy dissipative elements at RC structural wall, to achieve the target of low damage or no damage.[10-19]

Although some developments have been achieved on seismic resilience, few research results were related to the design philosophy for earthquake resilient structures and now no consensus on definition of seismic resilience of individual structures. So it is important to propose a consistent resilience target to evaluate the seismic resilience of individual existing structures and to design a new structure. Meanwhile, numerious aftershocks occur after the causative mainshock and the effects of aftershocks on the seismic resilience are significant. [20, 21] It is necessary to incorporate the aftershocks into the evaluation and design of structures from the point of view of resilience.

In this study, a resilience loss factor considering the recovery time and pre-event functionality is developed to incorperate the effects of aftershocks on the resilience of structure. The seismic resilience of a case-study reinforced concrete (RC) frame structure under mainshock-aftershock (MSAS) sequences is assessed by the proposed resilience loss factor.

2. Resilience assessment method

Resilience is generally defined as the ability of system to maintain or recover to the pre-event functionality after an earthquake. Resilience assessment considering the effects of aftershocks can be achieved by an indicator which can reflect the ability of system to maintain or recover to the pre-event functionality after an mainshock and aftershock sequence (MSAS).

According to Cimellaro et al. [23], the functionality for the MSAS case can be expressed as a function of earthquake intensity, economic loss, recovery time and recovery path represented by recovery function, as shown in Equation (1).

$$Q_{\mathrm{MSAS}}(t) = Q(t < t_0) - L(S_{\mathrm{a\_MS}}, \nabla S_{\mathrm{a}}, T_{\mathrm{RE}}) \cdot [H(t - t_0) - H(t - t_1)] \cdot f_{\mathrm{rec}}(t, t_0, T_{\mathrm{RE}}) \quad (1)$$

where $S_{\mathrm{a\_MS}}$ is the spectra acceleration of mainshock ground motion; ∇S_{a} is the relative S_{a} of aftershock ground motion, and it is defined as the ratio of spectra acceleration of aftershock ground motion to that of mainshock ground motion (i.e. $\nabla S_{\mathrm{a}} = S_{\mathrm{a\_AS}} / S_{\mathrm{a\_MS}}$) ; T_{RE} is the recovery time and it equals to t_1-t_0 (as shown in Figures 1 and 2); L is the loss function; H(t) is Heaviside step function; $f_{\mathrm{rec}}(t, t_0, T_{\mathrm{RE}})$ is the recovery function, and three possible recovery functions [23-25] are shown in Equation (2) below.

$$f_{\mathrm{rec}}(t, t_0, T_{\mathrm{RE}}) = \begin{cases} 1 - \dfrac{t - t_0}{T_{\mathrm{RE}}} & \text{linear} \\ \exp\left(-\dfrac{(t - t_0)(\ln 200)}{T_{\mathrm{RE}}}\right) & \text{exponential} \\ 0.5\left\{1 + \cos\left[\dfrac{\pi(t - t_0)}{T_{\mathrm{RE}}}\right]\right\} & \text{trigonometric} \end{cases} \quad (2)$$

We developed a resilience loss factor, which is normalized by the product of recovery time and pre-event

functionality $Q(t<t_0)$, to quantify the community earthquake loss of resilience based on the resilience loss factor proposed by Bruneau et al. [1], as shown in Equaiton (3). When considering the the effects of aftershocks, Equaiton (3) is further expressed as Equaiton (4).

$$R_{\text{loss\_MS}} = \frac{1}{[Q(t<t_0)]\cdot(t_1-t_0)}\int_{t_0}^{t_1}[Q(t<t_0)-Q_{\text{MS}}(t)]dt \tag{3}$$

$$R_{\text{loss\_MSAS}} = \frac{1}{[Q(t<t_0)]\cdot(t_1-t_0)}\int_{t_0}^{t_1}[Q(t<t_0)-Q_{\text{MSAS}}(t)]dt \tag{4}$$

t_1 is the time at which the functionality of a structure is recovered to $Q_{\text{target\_MS}}$; $Q_{\text{target\_MS}}$ is the functionality target for mainshock only case when the recovery process ends, and the value of $Q_{\text{target\_MS}}$ should be greater than or equal to the value of $Q(t<t_0)$ (i.e. $Q_{\text{target}} \geqslant Q(t<t_0)$). The lower value of $Q(t<t_0)$ can attribute to the functionality degradation induced by aging or other hazards previous earthquake. $Q(t)$ is the functionality of the structure after the mainshock, while $Q_{\text{MSAS}}(t)$ is the functionality of the structure after MSAS sequences; The value of $Q_{\text{MSAS}}(t_1)$ is smaller than that of $Q_{\text{target\_MS}}$ due to the effects of aftershocks.

Figure 1 illustrates the conceptual illustration for the resilience loss factor of mainshock (MS) and MSAS sequence. As shown in Figure 1(a), the area AB_1E minus the area EDD_1 is the resilience loss for the mainshock only. The area EDD_1 can be seen as the increased resilience by the higher target of recovery. The value of $R_{\text{loss\_MS}}$ in equation (3) is the ratio of the resilience loss (i.e. the result of the area AB_1E minus the area EDD_1) to the area ABCD. The value of Q_{target} is regarded to be 1.0 which is same with the value of $Q(t<t_0)$ for simplification, as demonstrated in Figure 1(b). Recovery path 2 make the structure recover more rapidly, so it leads to smaller value of R_{loss} than recovery paths 1 and 3.

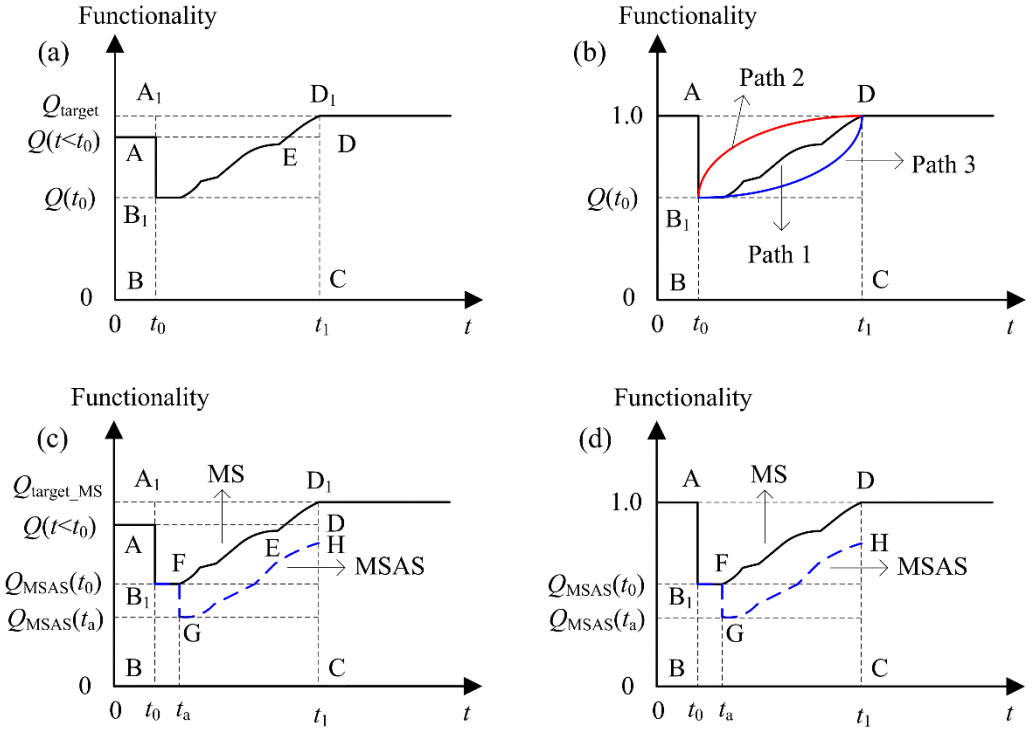

Figure 1. The conceptual illustration for the resilience loss factor of mainshock (MS) and MSAS sequence: (a) MS only, comprehensive case; (b) MS only, simplified case; (c) MSAS sequence, comprehensive case; (d) MSAS sequence, simplified case.

In Figure 1(c), the time t_a is the time point of an aftershock occurrence. $Q_{\text{MSAS}}(t_0)$-$Q_{\text{MSAS}}(t_a)$ represents the additional damage induced by the aftershock or effects of the aftershock on the usage of structure. The time

period of t_a-t_0 is the time gap between the mainshock and aftershock, and it is assumed that there is no increase on the functionality during this time gap. Due to the further reduction in functionality induced by the aftershock, the structure cannot be recovered to its pre-event functionality level at t_1 (i.e. $Q_{MSAS}(t_1) = Q(t<t_0)$) without additional repair work being performed. In order to quantify aftershock effects on the resilience loss, Equation (4) and Equation (3) share the same denominator. $[Q(t<t_0)]\cdot(t<t_0)$ is deemed to the nominal resilience capacity of a structure before an earthquake and used to normalize the resilience funtionality for both cases of only mainshock (MS) and MSAS sequence. Similarly, the illustration in Figure 1(c) can be further simplified to that in Figure 1(d) when the values of $Q(t<t_0)$ and Q_{target_MS} are both 1.0.

Figure 1 illustrates the resilience loss factor with the repair action after earthquakes. If the damage of a structure is beyond the threshold of repair, this structure would be demolished and a new one will be built. For example, many owners prefer to replace structures when the projected repair costs exceed about 40% or 50% of the replacement cost according to FEMA P-58 [22]. Therefore, if the economic loss reaches the threshold of replacement, the functionality $Q(t_0)$ and $Q_{MSAS}(t_a)$ are reduced to be zero and the replacement will be performed, as drawn in Figure 2. Then the values of R_{loss_MS} and R_{loss_MSAS} will become 1.0 because resilience is not meaningful any more for individual structures once the replacement is performed. The resilience loss factor can be defined comprehensively by Equation (5) for various cases.

$$R_{loss} = \begin{cases} \dfrac{1}{[Q(t<t_0)]\cdot(t_1-t_0)}\int_{t_0}^{t_1}[Q(t<t_0)-Q_{MS}(t)]dt & \text{repair} \quad R_{loss\_MS} \\ \dfrac{1}{[Q(t<t_0)]\cdot(t_1-t_0)}\int_{t_0}^{t_1}[Q(t<t_0)-Q_{MSAS}(t)]dt & \text{repair} \quad R_{loss\_MSAS} \\ 1.0 & \text{replace} \quad R_{loss\_MS} \quad R_{loss\_MSAS} \end{cases} \tag{5}$$

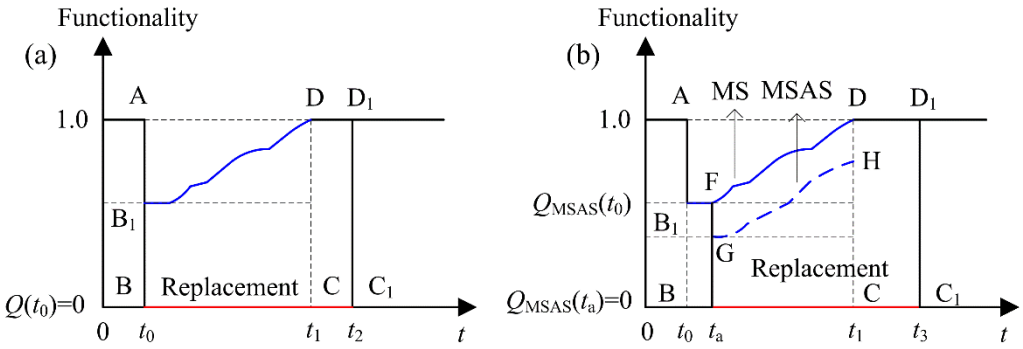

Figure 2. The conceptual illustration for the resilience loss factor of MS and MSAS sequence after considering the threshold of replacement: (a) MS only; (b) MSAS sequence.

3. Case Study Model

A 6-storey RC frame structure is used as the case study structure to apply the proposed resilience loss factor. The reinforced concrete (RC) frame structure has 6 stories and 3 bays and is designed to be located at the site II with intensity seven (i.e. the design peak ground acceleration is 0.1 g) according to the current Chinese building codes [26, 27]. The plane view and elevation of this structure is demonstrated in Figure 3. The reinforcement details and the section geometry of columns and beams are shown in Table 1. The dead and live loads are 5.0 kN/m^2 and 2.5 kN/m^2, respectively. The compressive strength of concrete for beam and column are 30 MPa and 35 MPa, respectively. The yield strength of longitudinal reinforcement and stirrup reinforcement are 400 MPa and 300 MPa, respectively.

The 2-Dimension frame structure in Figure 3 is modeled with the OpenSees [28] to assess the resilience loss of this structure under the MSAS sequences. The fundamental vibration period is 0.91 s for the bare frame

that analyzed in this study. The columns and beams are modelled by the displacement-based beam-column element with nonlinear fiber section. The concrete and steel behavior are modeled with Concrete02 material and Steel02 material. The bar-buckling and shear failure modes are not specially considered.

Table 1. The section geometry of columns and beams, as well as reinforcement details.

	Section		Longitudinal	Stirrup
	Width (mm)	Height (mm)	reinforcement (mm^2)	reinforcement
Edge beam	250	500	Top 1140 (3Φ22)	Φ8@100/150
			bottom 760 (2Φ22)	
Middle beam	250	400	Top 1140 (3Φ22)	Φ8@100/150
			bottom 760 (2Φ22)	
Column	500	500	2513 (8Φ20)	Φ8@100/150

274 MSAS ground motions, in which only one aftershock is contained, are used. Structual seismic demand is obtained by the increment dynamic analysis of MSAS sequences. For each MSAS sequence in the dataset, the S_a of mainshock ground motion S_{a_MS} is firstly scaled from 0.1 g to 1.2 g with an interval of 0.1 g. For each scaled mainshock ground motion, the relative intensity ∇S_a of the corresponding aftershock ground motion is scaled to 0.5, 0.8 and 1.0 respectively.

The fragility curves are computed for various cases based on the framework developed in [29]. The structual damage is quatified by the maximum inter-storey drift ratio (*MIDR*). The structual damage state is determined by four threthold of *MIDR*. The value ranges of *MIDR* for different damage status of structure are summarized in Table 2, and corresponding information on the direct economic loss ratio is also provided based on the Chinese code for the post-earthquake field works [30, 31]. The construction cost of the case study building is 371 million Chinese Yuan (CNY) according to the construction project cost information provided by the department of housing and urban-rural development of China.

Table 2. The values of maximum inter-storey drift ratio (*MIDR*) and direct economic loss ratio for various damage states of structure [31].

MIDR（%）	Damage state	Direct economic loss ratio (%)
IDR<1.0	DS_1: Minor damage	10
1.0≤*IDR* <2.0	DS_2: Moderate damage	40
2.0≤*IDR* <4.0	DS_3: Severe damage	70
4.0≤*IDR*	DS_4: Collapsed	100

4. Resilience Results and Discussion

The fragility curves of the structure for three limit states and different relative intensities of aftershock ground motions based on the framework in [29] is shown in Figure 4. Aftershock increases the seismic demand of structure compared with mainshock only. The probability of exceeding a give limit state is higher for MSAS sequence than for mainshock only, and the fragility curves are simply shifted up for the MSAS sequence cases.

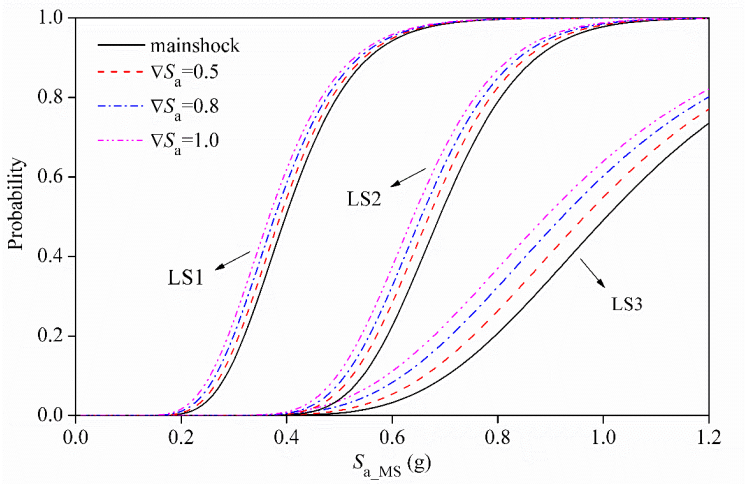

Figure 4. The fragility curves of the RC frame structure under the MSAS sequences.

The direct economic loss can be obtained by Equation (6), which considers the losses for various discrete damage states and for a given MSAS sequence intensity.

$$L_{\text{dir}} = \sum_{i=1}^{4} V \cdot R_{\text{DS}i} \cdot P(\text{DS}_i \,|\, IM) \tag{6}$$

V is the cost of building and it is 371 million CNY for this case-study building; $R_{\text{DS}i}$ is direct economic loss ratio corresponding to the ith damage state (as shown in Table 2); $P(DS_i \,|\, IM)$ is the probability of building experiencing the ith damage state for the given intensity measure, and it can be computed as:

$$P(DS_i \,|\, IM) = \begin{cases} F(DS_i \,|\, IM) - F(DS_{i+1} \,|\, IM) & i < 4 \\ F(DS_i \,|\, IM) & i = 4 \end{cases} \tag{7}$$

where $F(DS_i \,|\, IM)$ is the probability of exceeding ith damage state for the given intensity measure.

The direct economic loss results for mainshock only and MSAS sequences are shown in Figure 5. It is clear that aftershocks increase the direct economic loss. Larger intensity aftershock tends to incur greater loss. The direct economic loss is used to compute the loss function of Equation (1), and the functionality of this building is reflected by the direct economic loss. The loss function is the ratio of direct economic loss to the building replacement cost as defined in reference [2]. Building replacement cost used in this study is 1.25 times of the initial construction cost. The replacement will be performed when the repair cost exceeds the 45% of building replacement cost where the direct economic loss is used as repair cost. The linear recovery function is used for the average prepared community.

Figure 6(a) illustrates the variation of $R_{\text{loss\_MS}}$ with the increase of $S_{\text{a\_MS}}$ for the cases with and without consideration of replacement threshold and Figure 6(b) shows the variation of $R_{\text{loss\_MSAS}}$ with the increase of $S_{\text{a,ms}}$ for the case with consideration of replacement threshold. In Figure 6(a), the difference turing point is at $S_{\text{a,MS}}$=0.64g with and without consideration of replacement threshold. Considering the replacement threshold increases the resilience loss of structure by the minimum level of 200% when the replacement threshold is reached. This phenomenon also highlights that the recovery path has significant effects on the values of resilience loss factor. In Figure 6(b), aftershocks with larger intensities make the $S_{\text{a\_MS}}$ corresponds to replacement threshold minimized, and the $S_{\text{a\_MS}}$ decreases from 0.64 g to 0.59 g for ∇S_{a}=1.0 g and mainshock only. The effects of aftershocks on the resilience loss exceed 400% when the replacement threshold is reached.

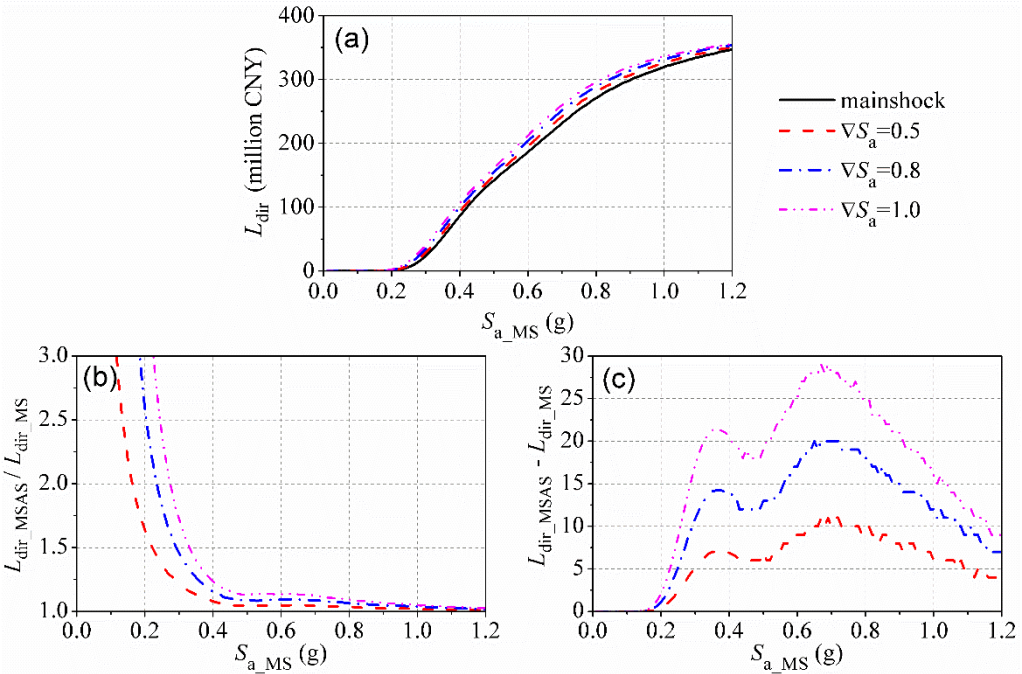

Figure 5. Direct economic loss L_{dir} induced by MSAS sequences and effects of aftershocks: (a) L_{dir} (million CNY); (b) L_{dir_MSAS} / L_{dir_MS}; (c) L_{dir_MSAS} - L_{dir_MS} (million CNY).

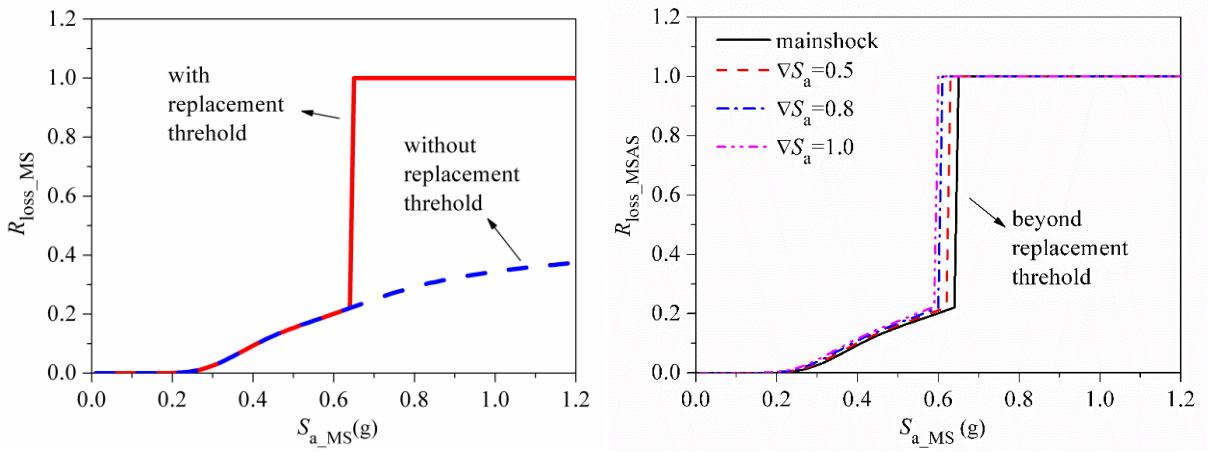

Figure 6. The variation of R_{loss} with the increase of S_{a_MS} :(a) cases for mainshock only with and without consideration of replacement threshold; (b) cases for mainshock only and 3 MSAS with consideration of replacement threshold.

5. Conclusion

A resilience loss factor by introducing the normalization by the product of the recovery time and pre-event functionality is developed. The resilience loss factor is extended to incorporate the effects of aftershocks by including the further reduction in functionality induced by aftershock. The replacement threshold based on the repair cost is also incorporated to reflect the engineering application.

A case-study reinforced concrete (RC) frame structure under mainshock-aftershock (MSAS) sequences is used for resilience loss factor applicaiton. Considering the replacement threshold increases the resilience loss of structure by the minimum level of 200% when the replacement threshold is reached. Aftershock can increase the resilience loss with respect to the mainshock alone, and the proposed resilience loss factor can

reflect the effects of aftershocks. The effects of aftershocks on the resilience loss exceed 400% when the replacement threshold is reached.

6. Acknowledgements

The authors want to appreciate the supports from the National Natural Science Foundation of China (51708161, 51825801, and 51938004). The underground motion data were collected from Kik-net stations, and the operation work by NIED is greatly appreciated.

7. References

[1] Bruneau M, Chang S E, Eguchi RT, et al. A framework to quantitatively assess and enhance the seismic resilience of communities. Earthquake spectra 2003; 19(4): 733-752.
[2] Cimellaro GP, Reinhorn AM, Bruneau M. Framework for analytical quantification of disaster resilience. Engineering Structures 2010; 32(11): 3639-3649.
[3] Cimellaro GP, Christovasilis IP, Reinhorn AM, et al. L'Aquila earthquake of April 6th, 2009 in Italy: rebuilding a resilient city to multiple hazard. MCEER Technical Rep.—MCEER-10, 2010, 10.
[4] Cimellaro GP, Reinhorn AM, Bruneau M. Performance-based metamodel for healthcare facilities. Earthquake Engineering & Structural Dynamics 2011; 40(11): 1197-1217.
[5] Miles SB, Chang SE. Urban disaster recovery: A framework and simulation model. MCEER-03-0005, Multidisciplinary Center for Earthquake Engineering Research, Buffalo, NY. 2003.
[6] Miles SB, Chang SE. Modeling community recovery from earthquakes. Earthquake Spectra 2006; 22(2), 439–458.
[7] Miles SB, Chang SE. A simulation model of urban disaster recovery and resilience: Implementation for the 1994 Northridge earthquake. MCEER-07-0014, Multidisciplinary Center for Earthquake Engineering Research, Buffalo, NY. 2007.
[8] Miles SB, Chang SE. ResilUS: A community based disaster resilience model. Cartography and Geographic Information Science 2011; 38(1): 36-51.
[9] Cimellaro GP, Tinebra A, Renschler C, et al. New resilience index for urban water distribution networks. Journal of Structural Engineering 2015; 142(8): C4015014.
[10] Deierlein G, Krawinkler H, Ma X, et al. Earthquake resilient steel braced frames with controlled rocking and energy dissipating fuses. Steel Construction 2011; 4(3): 171-175.
[11] Sabbagh AB, Petkovski M, Pilakoutas K, et al. Experimental work on cold-formed steel elements for earthquake resilient moment frame buildings. Engineering Structures 2012; 42: 371-386.
[12] Mayes RL, Brown AG, Pietra D. Using seismic isolation and energy dissipation to create earthquake-resilient buildings. Bulletin of the New Zealand Society for Earthquake Engineering 2012; 45(3): 117-122.
[13] Rodgers GW, Mander JB, Chase JG, et al. Beyond ductility: parametric testing of a jointed rocking beam-column connection designed for damage avoidance. Journal of Structural Engineering 2016; 142(8): C4015006.
[14] Liu Q, Jiang H. Experimental study on a new type of earthquake resilient shear wall. Earthquake Engineering & Structural Dynamics 2017; 46(14): 2479–2497.
[15] Bachmann JA, Vassiliou MF, Stojadinović B. Dynamics of rocking podium structures. Earthquake Engineering & Structural Dynamics 2017; 46(14): 2499-2517.
[16] Roh H, Reinhorn AM. Nonlinear static analysis of structures with rocking columns. Journal of structural engineering 2010; 136(5): 532-542.
[17] Anastasopoulos I, Kourkoulis R, Gelagoti F, et al. Rocking response of SDOF systems on shallow improved sand: An experimental study. Soil Dynamics and Earthquake Engineering 2012; 40: 15-33.
[18] Anastasopoulos I, Drosos V, Antonaki N. Three-storey building retrofit: rocking isolation versus conventional design. Earthquake Engineering & Structural Dynamics 2015; 44(8): 1235-1254.
[19] Vassiliou MF, Truniger R, Stojadinović B. An analytical model of a deformable cantilever structure rocking on a rigid surface: development and verification. Earthquake Engineering & Structural Dynamics 2015; 44(15): 2775-2794.
[20] Cimellaro GP, Solari D, Bruneau M. Physical infrastructure interdependency and regional resilience index after the 2011 Tohoku Earthquake in Japan. Earthquake engineering & structural Dynamics 2014; 43(12): 1763-1784.
[21] Dong Y, Frangopol DM. Risk and resilience assessment of bridges under mainshock and aftershocks incorporating uncertainties. Engineering Structures 2015; 83: 198-208.
[22] FEMA P-58-1: Seismic Performance Assessment of Buildings. Volume 1–Methodology. 2012.
[23] Cimellaro GP, Reinhorn AM, Bruneau M. Seismic resilience of a hospital system. Structure and Infrastructure Engineering 2010; 6(1-2): 127-144.

[24] Kafali C, Grigoriu M. Rehabilitation decision analysis. In: ICOSSAR'05, Proceedings of the 9th international conference on structural safety and reliability, 19–23 June, Rome, Italy, 2005.
[25] Chang S,Shinozuka M. Measuring improvements in the disaster resilience of communities. Earthquake Spectra2004; 20 (3): 739–755.
[26] Ministry of Housing and Urban-Rural Development of P. R. China. Code for design of concrete buildings, GB 50010-2010. China Architecture and Building Press, Beijing, China, 2010.
[27] Ministry of Housing and Urban-Rural Development of P. R. China. Code for seismic design of buildings, GB 50010-2010.
[28] OpenSees. Open system for earthquake engineering simulation. http://opensees.berkeley.edu/.
[29] Wen W, Zhai C, Ji D, Li S, Xie L. Framework for the vulnerability assessment of structure under mainshock-aftershock sequences. Soil Dynamics and Earthquake Engineering 2017; 101: 41-52.
[30] FEMA-356. Prestandard and commentary for the seismic rehabilitation of buildings. FEMA, 2000.
[31] China national standardization management committee. Post-earthquake field works-part 4: assessment of direct loss. GB/T 18208.4, 2011.

